Chemosphere 224 (2019) 658–667

Contents lists available at ScienceDirect

Chemosphere

journal homepage: www.elsevier.com/locate/chemosphere

Uptake and toxicity studies of magnetic TiO_2-Based nanophotocatalyst in *Arabidopsis thaliana*

Weilan Zhang [a], Zhigang Yu [a], Pinhua Rao [b, **], Irene M.C. Lo [a, c, *]

[a] Department of Civil and Environmental Engineering, The Hong Kong University of Science and Technology, Hong Kong, China
[b] School of Chemistry and Chemical Engineering, Shanghai University of Engineering Science, Shanghai, 201620, China
[c] Institute for Advanced Study, The Hong Kong University of Science and Technology, Hong Kong, China

HIGHLIGHTS

- N-TiO_2/Fe_3O_4@SiO_2 (NTFS) nanophotocatalyst can be taken up by *Arabidopsis* root and transported to plant leaves.
- NTFS did not cause any changes in the lipids, pectins, proteins, cellulose, hemicellulose, and carbohydrates.
- NTFS did not alter the morphology and biomass of *Arabidopsis*.
- The energy physiology of *Arabidopsis* was not affected by NTFS.

GRAPHICAL ABSTRACT

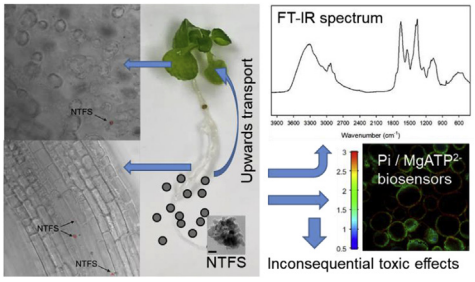

ARTICLE INFO

Article history:
Received 5 January 2019
Received in revised form
18 February 2019
Accepted 22 February 2019
Available online 28 February 2019

Handling Editor: Daniel CW Tsang

Keywords:
Arabidopsis thaliana
Biosensor
Magnetic nanophotocatalyst
Titanium dioxide

ABSTRACT

Information on the environmental impact of magnetic TiO_2-based nanophotocatalysts is scarce. This study evaluated the potential effects of an innovative magnetic nanophotocatalyst N-TiO_2/Fe_3O_4@SiO_2 (NTFS) on plants using *Arabidopsis thaliana* grown in a hydroponic system. NTFS was detected in the vascular tissues and mesophyll of plants, thus confirming the uptake and upwards transport of NTFS from roots to leaves. Fourier transform infrared spectroscopy was applied to determine compositional and structural alterations in plant tissues exposed to NTFS, or its two main components (N-TiO_2 and Fe_3O_4@SiO_2), at concentrations ranging from 0 to 1000 mg/L, but no changes were detected in the lipids, pectins, proteins, cellulose, hemicellulose, and carbohydrates. The morphology and biomass of the plants were not affected by the NTFS or its components either. Biosensors for inorganic phosphate (Pi) and $MgATP^{2-}$ were used to monitor the in vivo Pi and $MgATP^{2-}$ levels in the plant cells. The results showed that NTFS and its components did not induce any adverse effects on the cytosolic Pi level or ATP synthesis, indicating the energy physiology of *Arabidopsis* was unaffected. In general, NTFS has inconsequential toxic effects on *Arabidopsis*, but can be taken up by plants, enter the food chain, and cause potential exposure and bioaccumulation in animals and human beings.

1. Introduction

Titanium dioxide nanoparticle (TiO_2NP) is one of the most widely investigated candidates for photocatalytic degradation of organic pollutants due to its efficient degradation performance, biological and chemical stability, and low cost (Asahi et al., 2014;

* Corresponding author. Department of Civil and Environmental Engineering, The Hong Kong University of Science and Technology, Hong Kong, China.
** Corresponding author.
E-mail addresses: raopinhua@hotmail.com (P. Rao), cemclo@ust.hk (I.M.C. Lo).

https://doi.org/10.1016/j.chemosphere.2019.02.161
0045-6535/

Schneider et al., 2014). In recent years, tremendous efforts have been made to further improve the visible-light photocatalytic performance and introduce magnetic properties to TiO_2NPs for material recovery and reuse. For example, nitrogen-doping method was widely applied in TiO_2NP modification to shift the photon absorption of TiO_2 from the UV region into the visible-light region, allowing the efficient utilization of solar energy (Burda et al., 2003; Chen and Burda, 2008). To bring in magnetic property, Fe_3O_4 nanoparticles were usually selected to blend into the TiO_2-based nanostructures and SiO_2 was thereby introduced to protect Fe_3O_4 from oxidation. Based on the analysis using Web of Science, 684 peer reviewed research articles on the topic of synthesis and applications of TiO_2/Fe_3O_4 magnetic nanocomposites have been published during the last five years (search topic=(TiO_2) AND (Fe_3O_4) AND (nanoparticles OR nanocomposite)). Among them, there are 191 papers specifically investigated the $TiO_2/Fe_3O_4@SiO_2$ nanocomposites, implying the research directions of TiO_2-based nanophotocatalysts. Besides the extensive laboratory investigations, TiO_2-based photocatalysts also have applications in practice. For example, TiO2-based photocatalysts were used to deodorize the indoor air contaminated by formaldehyde at low concentration (Aïssa et al., 2011). TiO_2-based photocatalysts were also successfully applied for the degradation of dyes (e.g., indigo, indigo carmine) and other organic pollutants (e.g. benzene, benzofuran, dichlorophenoxyacetic acid) in wastewater (Herrmann et al., 1998; Vautier et al., 2001; Rao et al., 2007; Akpan and Hameed, 2009; Xu et al., 2010). Previously, we also developed N-$TiO_2/Fe_3O_4@SiO_2$ (NTFS), which is a typical magnetic TiO_2-based nanophotocatalyst and could effectively degrade pharmaceuticals and personal care products (PPCPs) under visible light (Kumar et al., 2017). The recovery efficiency of the nanophotocatalyst from treated water could be up to 95% after magnetic separation.

Due to the promising potential of using visible light driven magnetic TiO_2-based nanophotocatalysts for organic pollutant removal, their environmental-related applications in full-scale are foreseeable. The incidental or direct release/disposal of the nanophotocatalysts into the environment as an emerging contaminant thereby need concerns, considering the potential eco-toxicological risks. Unfortunately, to date, few studies have investigated the toxicological and environmental effects of direct and indirect exposure to these emerging materials and no clear guidelines exist to quantify these effects. Plants are an essential base component of all ecosystems and have high chance to be directly exposed to the contaminants in aqueous or soil systems. Thus, plants have played an important role in the fate and transport of engineered nanoparticles in the environment through plant uptake and bioaccumulation (Monica and Cremonini, 2009). An important aspect of the risk assessment of TiO_2-based nanophotocatalysts is thereby to understand the interactions of the nanophotocatalysts with plants. Numerous reports have recently been published on the phytotoxicity of traditional non-magnetic TiO_2NPs. For instance, the toxicity of pure TiO_2NPs has been tested on tobacco (Ghosh et al., 2010), willow trees (Seeger et al., 2009), onions (Ghosh et al., 2010; Klančnik et al., 2011), rice (Ma et al., 2017), and spinach (Hong et al., 2005; Lei et al., 2007). Fe_3O_4 nanoparticles, which introduce magnetic properties to the nanophotocataylysts, could induce oxidation stress to plants (Wang et al., 2011) and may change the toxicology of non-magnetic TiO_2NPs. However, none of the previous publications focused on the uptake and phytotoxicities of visible light driven magnetic TiO_2-based nanophotocatalysts, which are becoming more mainstream in organic pollutant removal studies (Chen et al., 2008; Xuan et al., 2008; Chalasani and Vasudevan, 2013). The lack of information on plant uptake and phytotoxicity may hinder the process of using these recyclable materials from laboratory experiments to full-scale applications. Therefore, a sound evaluation of the interactions between plants and visible light driven magnetic TiO_2-based nanophotocatalysts is necessary to bridge this knowledge gap.

The phytocixity of nanoparticles can be studied in terms of the cytosolic levels of inorganic phosphate (Pi) and adenosine triphosphate (ATP), which are important indexes of plant metabolism and growth (Mukherjee et al., 2015; De Col et al., 2017). For example, the phosphate-dependent metabolism, including the synthesis of nucleic acid and ATP, photosynthesis, and enzyme activity regulation, is strongly correlated to the cytosolic Pi level (Vance et al., 2003). ATP is the universal cellular energy source providing energy to plant life processes (Knowles, 1980). As the building block and energy source of cell membranes, cell walls, proteins, and carbohydrates biosynthesis, the changes of cytosolic Pi and ATP levels could be reflected through the compositional and structural alterations in plant tissues. Fourier Transform Infrared (FT-IR) spectroscopy is a powerful tool for gathering chemical information from a growing and developing plant and has been used to identify compositional and structural changes of lipids, cell wall components, proteins, and carbonhydrates in previous studies (Knowles, 1980; Vance et al., 2003; Dokken et al., 2005; Rico et al., 2015). Zahra et al. (2015) reported that TiO_2NPs (12–20 nm, 0–250 mg/kg in soil) could affect the plant uptake of phosphorus, hence could potentially influence the plant cytosolic Pi level and consequential ATP synthesis. A series of investigations on the growth enhancement of spinach exposed to TiO_2NPs (anatase, up to 6% in water) and its mechanism reveals that TiO_2NPs could promote chlorophyll biosynthesis and photosynthesis, enhance the activities of Mg^{2-}ATPase, and potentially affect the ATP level in plant tissues of spinach (Hong et al., 2005; Lei et al., 2007). However, due to technical limitations, the cytosolic levels of Pi and ATP have not been investigated directly to provide the required deep insights into the possible changes in plants caused by TiO_2-based nanophotocatalysts. The latest technique in expressing biosensors for Pi and $MgATP^{2-}$ in *Arabidopsis thaliana* enables the monitoring of the cytosolic Pi and ATP levels in plant cells (Mukherjee et al., 2015; De Col et al., 2017). By studying the biosensors, the effects of magnetic TiO_2-based nanophotocatalysts on the cytosolic Pi and ATP levels could yield important information regarding their phytotoxicity.

In this study, NTFS, which a typical visible light driven magnetic TiO_2-based photocatalyst, was selected due to its promising degradation performance, and recyclability (Kumar et al., 2017). A hydroponic study was conducted with *Arabidopsis* plants with either cytosolic Pi biosensors (cpFLIPPi-6.4 m) or cytosolic $MgATP^{2-}$ biosensors (ATeam1.03-nD/nA). Compositional and structural changes of plant tissues exposed to NTFS were identified using FT-IR spectroscopy. The Pi and $MgATP^{2-}$ levels in the cytosol of living plants exposed to NTFS were determined by analyzing the fluorescent proteins (Pi and $MgATP^{2-}$ biosensors) in the plant tissues. To provide an insight into the plant uptake and phytotoxicity of magnetic TiO_2-based nanophotocatalysts, the specific objectives of this study are (1) to determine the uptake of NTFS by *Arabidopsis*; (2) to investigate compositional and structural alterations in plant tissues after exposure to NTFS; and (3) to study the impacts of NTFS on the inorganic phosphate and ATP levels in plant cells.

2. Materials and methods

2.1. Reagents

The chemical reagents used in this study, including $FeCl_3 \cdot 6H_2O$, $FeCl_2 \cdot 4H_2O$ $Na_2HAsO_4 \cdot 7H_2O$, $NH_3 \cdot H_2O$, trisodium citrate dehydrate, tetraethyl orthosilicate, titanium butoxide, potassium hydroxide, calcium chloride, nitric acid, hydrogen peroxide, alizarin red S, and Murashige and Skoog salt mixture, were purchased from

Sigma-Aldrich (St. Louis, MO, USA).

2.2. Nanoparticle synthesis and characterization

NTFS and its two main components (nitrogen-doped N-TiO_2 and Fe_3O_4@SiO_2) were synthesized following the modified methods published by Kumar et al. (2017) The detailed methods are shown in the supplementary materials. The morphology, size, and elemental composition of the materials were analyzed by a TM3030 scanning electron microscope (SEM) equipped with energy dispersive X-ray spectroscopy (Hitachi, Japan). The size distributions of all the nanoparticles in the TEM images (Fig. 1) are shown in Fig. S1. The average size of the NTFS nanoparticles was 35.12 ± 5.72 nm. The sizes of the two components, NT and FS, were 17.57 ± 2.68 and 23.89 ± 3.51 nm, respectively. The elements Ti, Fe, Si, and O were all detected using EDS, indicating successful Fe_3O_4@SiO_2 and NTFS synthesis (Fig. 1). The Ti content in the NTFS were determined using a Varian 725-ES Inductively Coupled Plasma-Optical Emission Spectrometer (ICP-OES) (Mulgrave VIC, Australia) after acid digestion (Mudunkotuwa et al., 2016). The mass percent of Ti in NTFS measured by ICP-OES was 56.48 ± 4.97%. The calculated mass ratio of NT to FS in NTFS was approximately 65:35.

2.3. Exposure of Arabidopsis seedlings to NTFS, N-TiO_2, and Fe_3O_4@SiO_2

The transgenic *Arabidopsis* seeds expressing cytosolic Pi biosensor (cpFLIPPi-6.4 m) or cytosolic $MgATP^{2-}$ biosensor (ATeam1.03-nD/nA) were germinated following the method published by Zhang et al. (2018). The surface of seeds was first sterilized by 70% (v/v) ethanol, followed by 10% (v/v) bleach (active ingredient: sodium hypochlorite) for 2 min. Afterwards, the seeds were washed by DI water for 5 times and transferred to half-strength Murashige and Skoog medium (MS medium) (Murashige and Skoog, 1962) with 0.25% (w/v) sucrose at 4 °C. The ingredients of the MS medium are shown in Table S1. After 2 days, the stratified seeds were transferred to a 96-well plate containing 0.25 mL of the MS medium with 0.25% (w/v) sucrose in each well. The 96-well plate was incubated with a 16 h light/8 h dark cycle (LED grow light, 30 W) at 22 °C. The germination rate of the *Arabidopsis* seeds was higher than 99% in this hydroponic study. After 6 days, the *Arabidopsis* seedlings in the 96-well plate were transferred to a new 96-well plate and exposed to NTFS at different concentrations, respectively. The pH of all growth media was adjusted to 5.7–5.8 using potassium hydroxide. The dosage of TiO_2-based photocatalysts for the organic pollutant degradation in previous publications was up to 1000 mg/L (Álvarez et al., 2010; Kumar et al., 2017). Considering the worst scenario (all materials in the treated water were failed to recover and expose to plants directly), the highest concentration of NTFS in this study was set at 1000 mg/L, which is also a typical dose used in the phytotoxicity studies of TiO_2-based nanophotocatalys (Lei et al., 2007; Chen et al., 2008; Ghosh et al., 2010; Zahra et al., 2015). In order to gain an in-depth understanding of the toxicity of NTFS, the effects of the two main components of NTFS (NT and FS) on the *Arabidopsis* were also assessed. The concentrations of NT and FS were set up based on the mass ratio of NT to FS in NTFS. The medium used in this study was

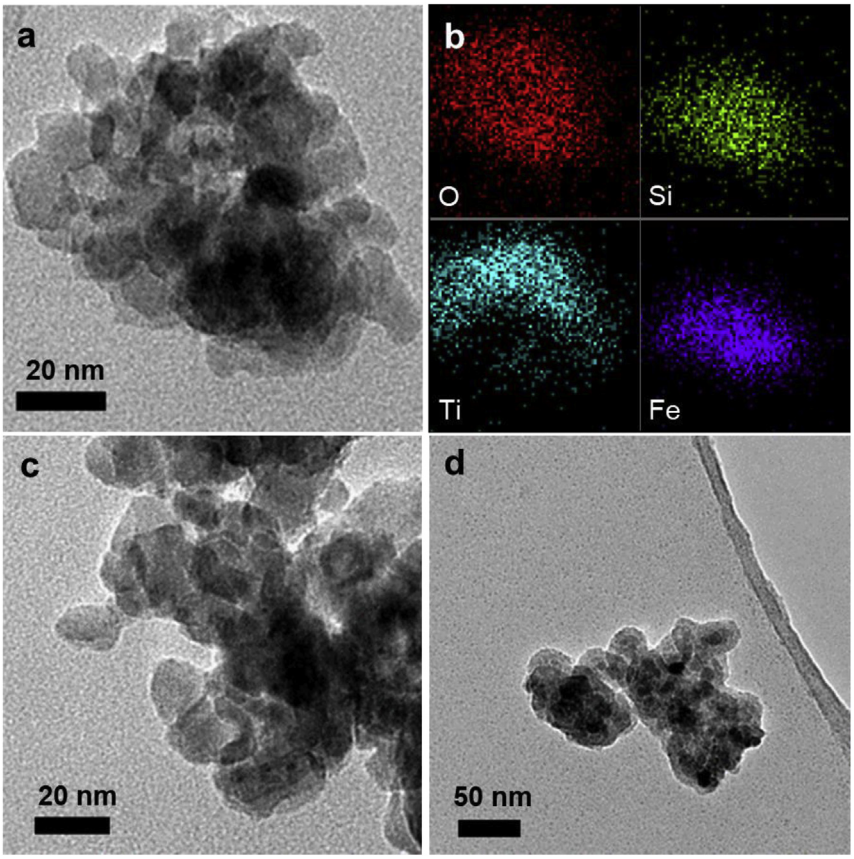

Fig. 1. (a) TEM image and (b) elemental mapping information of N-TiO_2/Fe_3O_4@SiO_2 nanophotocatalyst (NTFS), and TEM images of (c) N-TiO_2 nanoparticles (NT) and (d) Fe_3O_4@SiO_2 nanoparticles (FS).

half-strength MS medium containing 0.25% (w/v) sucrose and the treatments were prepared as follows. T1: Medium only. T2-4: Medium with NTFS at three concentrations (100, 500, and 1000 mg/L). T5-T7: Medium with N-TiO_2 (NT) at three concentrations (65, 325, and 650 mg/L). T8-T10: Medium with Fe_3O_4@SiO_2 (FS) at three concentrations (35, 175, and 350 mg/L). To maintain the pH of growth media at 5.7–5.8, all health Arabidopsis seedlings were rinsed by deionized water before transferring. Each treatment had 16 replicated plants.

2.4. Determination of Ti and Fe concentrations in plant tissues

After 5 days of exposure to NTFS, NT, and FS particles, *Arabidopsis* plants were sacrificed for the determination of Ti and Fe concentrations. In order to remove the adhering particles on the plant surface, entire plants were first rinsed by $CaCl_2$ solution at 5 mM for five times and then washed by DI water. The harvested plants were then freeze-dried for 72 h. The fresh and dry biomass of three representative plants from each treatment was recorded before and after freeze-drying. The dry plants (three plants in each treatment) were then digested using strong acid following a previously developed procedure (Song et al., 2013). The freeze-dried tissues were mixed with 3 mL of 70% (v/v) nitric acid and digested at 80 °C for 2 h. After cooling to room temperature, 1 mL of 30% (w/v) perchloric acid was added to the mixture. The solution was heated to 200 °C until it became clear. The total Ti and Fe concentrations in the digest were quantified using ICP-OES.

2.5. Confocal microscopy imaging of the NTFS uptake by plants

The vicinal hydroxyl groups of Alizarin Red S (ARS) are able to bind TiO_2 (Fig. S2a) (Puchtler et al., 1969; Thurn et al., 2009; Blatnik et al., 2012). Thus, ARS can be used to label and track the NTFS particles. To surface modify NTFS, ARS (60 μM) was mixed with NTFS (1000 mg/L). The samples were then analyzed under a Zeiss LSM710 confocal microscope (Oberkochen, Germany). The original NTFS and the ARS labeled NTFS were excited by laser at 543 nm. The fluorescence was measured at 560–615 nm. Figs. S2b and c shows the confocal images of the original and ARS labeled NTFS, indicating the success of NTFS labeling with ARS.

On the 6th day after germination, *Arabidopsis* plants were exposed to the medium with labeled NTFS at 1000 mg/L for another 5 days to study the uptake and distribution of NTFS. On the 5th day after exposure, the root and leaf tissues were examined using a confocal microscope. A laser excitation wavelength of 543 nm was used. Emission was collected using a 560–615 nm band-pass filter. For each sample, serial scanning along the z-axis of the sample was conducted to obtain 3-D images, and the number of scanning planes was 34. The distance between two optical planes was approximately 1 μm.

2.6. FT-IR analysis

Changes in lipids, lignin, proteins, and carbohydrates were studied by using FT-IR spectroscopy. Five milligrams of freeze-dried

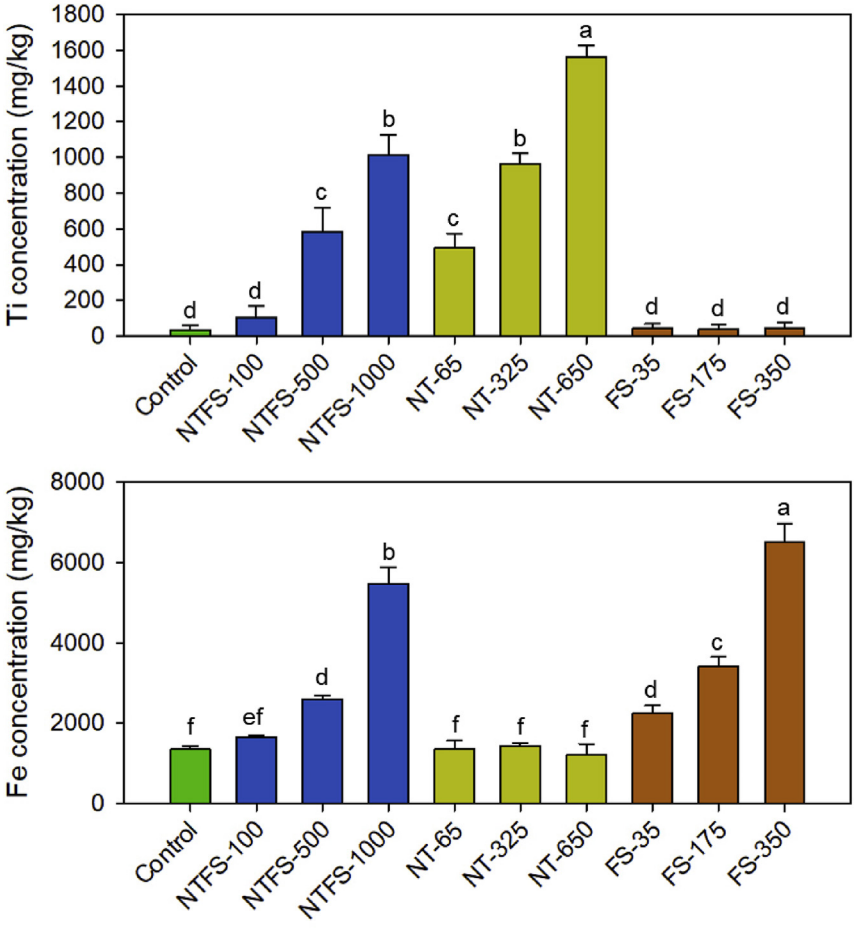

Fig. 2. (a) Total Ti and (b) total Fe concentrations (mg element/kg dry plant tissue) in whole plant seedlings on the fifth day of exposure to different treatments. Error bars represent standard deviations (n = 3). Different letters in lower case represent significant differences between the treatments in a one-way ANOVA followed by the Tukey test ($p < 0.05$).

plant tissues from each treatment were mixed with 100 mg of potassium bromide and ground to fine particles. Afterwards, the mixture was compressed in a pellet press to form a pellet for FT-IR analysis. Infrared analysis was performed using a Vertex 70 Hyperion 1000 FT-IR spectrophotometer (Bruker, Billerica, MA, USA). The spectral resolution was 4 cm^{-1} and the spectral range was 400 cm^{-1} to 4000 cm^{-1}.

2.7. Assessment of cytosol Pi and $MgATP^{2-}$ levels

On the 10th after germination (5 days of exposure to NTFS, NT, and FS particles), three healthy *Arabidopsis* plants were randomly selected from each treatment and studied under a confocal microscope (LSM710, Zeiss, Oberkochen, Germany) following the developed protocol (Zhang et al., 2018). Briefly, the Pi biosensor and the $MgATP^{2-}$ biosensor were excited at 458 nm. The excited biosensors in the mesophyll cells of intact leaves could generate fluorescence emissions at 465–500 nm (mseCFP (CFP)) and 526–561 nm (cp173-mVenus (Venus)), which were measured by confocal microscope. For each plant replicate, 3 images were generated from the cotyledon of *Arabidopsis*. The Redox Ratio Analysis software developed by Fricker (2016) was used to process the collected confocal images and calculate the ratio of Venus to CFP, which represents the cytosol Pi or $MgATP^{2-}$ level in the plants.

3. Results and discussion

3.1. The uptake and accumulation of NTFS

In this study, the elevated Ti concentrations in the plant tissues exposed to NTFS (Fig. 2a) indicate the uptake of NTFS by *Arabidopsis*. In general, the uptake of Ti by the plants increased with the increasing NTFS and the increasing N-TiO_2 (NT) concentrations. Similarly, the uptake of Fe increased with the increasing NTFS and the increasing Fe_3O_4@SiO_2 (FS) concentrations (Fig. 2b). The elevated concentrations of Ti and Fe in the plants exposed to NT and FS, respectively, imply the uptake of NT and FS nanoparticles by *Arabidopsis*. In the absence of NTFS and NT nanoparticles, the plants contained negligible amounts of Ti. However, the control plants and plants exposed to NT nanoparticles still had significant amounts of Fe in the plant tissues, because of the nutrient uptake ($FeSO_4 \cdot 7H_2O$) from the MS medium. Notably, although the total Ti concentrations in the hydroponic systems of NTFS-100, NTFS-500, and NTFS-1000 were theoretically equal to the corresponding Ti concentrations in the hydroponic systems of NT-65, NT-325, and NT-650, respectively, the Ti concentration in the plants exposed to NTFS were lower than in the corresponding plants exposed to NT (i.e. NTFS-100<NT-65, NTFS-500<NT-325, NTFS-1000<NT-650). The same trend was found for the Fe concentrations in plants exposed to NTFS and FS (i.e. NTFS-100<FS-35, NTFS-500<FS-175, NTFS-1000<FS-350). This is likely due to the larger average size of the NTFS heterostructure compared to NT and FS. The mean size of the magnetic nanophotocatalyst NTSF synthesized in this study was 35.12 ± 5.72 nm (Fig. 1), while the mean sizes of NT and FS were both less than or around 20 nm. Plant cells are surrounded by the cell walls, with pores that are believed to be in the 1–20 nm diameter range (Carpita et al., 1979; Nair et al., 2010). Nanoparticles with sizes smaller than or similar to the pore size are able to diffuse toward the plasma membrane, enter into the plant cells and accumulate in specific subcellular locations. Considering the pore

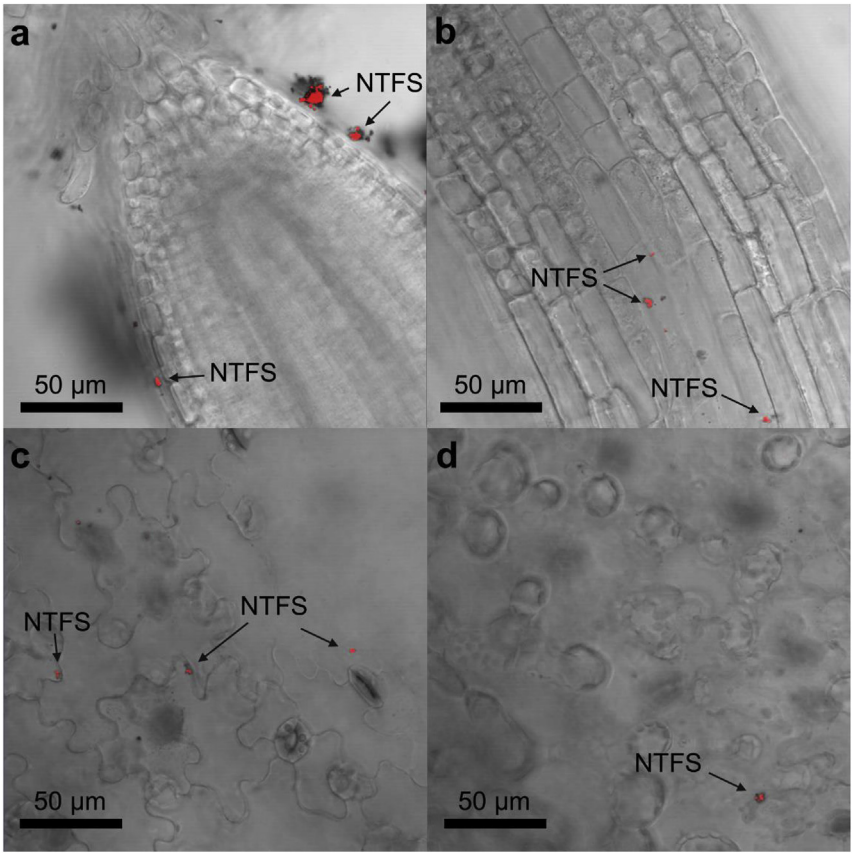

Fig. 3. Confocal microscopic images of the *Arabidopsis* seedlings on the fourth day of exposure to ARS stained NTFS at 1000 mg/L (the 10th day after germination): (a) root cap; (b) surface scan of root treated by NTFS; (c) epidermis of plant leaf; (e) mesophyll of plant leaf. The red signals were from the NTFS. (For interpretation of the references to color in this figure legend, the reader is referred to the Web version of this article.)

size, part of the NTFS exposing to the plants may be blocked by the cell walls, leading to the lower Ti and Fe concentrations compared to those in the corresponding plants exposed to NT or FS.

By staining with ARS, the labeled TiO_2NPs can be located in plant tissues under a confocal microscope using a 560–615 nm band-pass filter (excitation = 543 nm) (Thurn et al., 2009; Kurepa et al., 2010). Kurepa et al. (2010) reported that the ARS labeled TiO_2NPs (<5 nm) can be taken up by the *Arabidopsis* roots, translocated to the leaves, and randomly accumulated in the stomata pores. Fig. 3 shows the confocal images of *Arabidopsis* exposed to ARS labeled NTFS at a concentration of 1000 mg/L, captured on the surface and at different depths from the surface of the plant tissues. The aggregated NTFS particles were detected on the root surface (Fig. 3a) and in the vascular tissue of the plant roots (Fig. 3b). The 3-D confocal images of the plant roots exposed to ARS labeled NTFS further confirmed the penetration of NTFS into the root vascular tissue (Fig. S3). The results were consistent with the microscopic finding that NTFS can be taken up by *Arabidopsis*. Aggregated NTFS particles were also detected in the epidermis and the mesophyll of the plant leaves (Fig. 3c and d). Vascular tissue transports nutrients, water, and hormones within the plant, with the primary components of vascular tissue being the xylem and phloem. Larue et al., 2012a, 2012b found that TiO_2NPs can be absorbed by wheat roots and translocated to the vascular system without modification using micro X-ray fluorescence (micro-XRF) combined with micro X-ray Absorption Near Edge Structure (micro-XANES), suggesting that TiO_2NPs can potentially reach edible portions of the crop plants (leaves or fruits) and pose a threat for human health. The detection

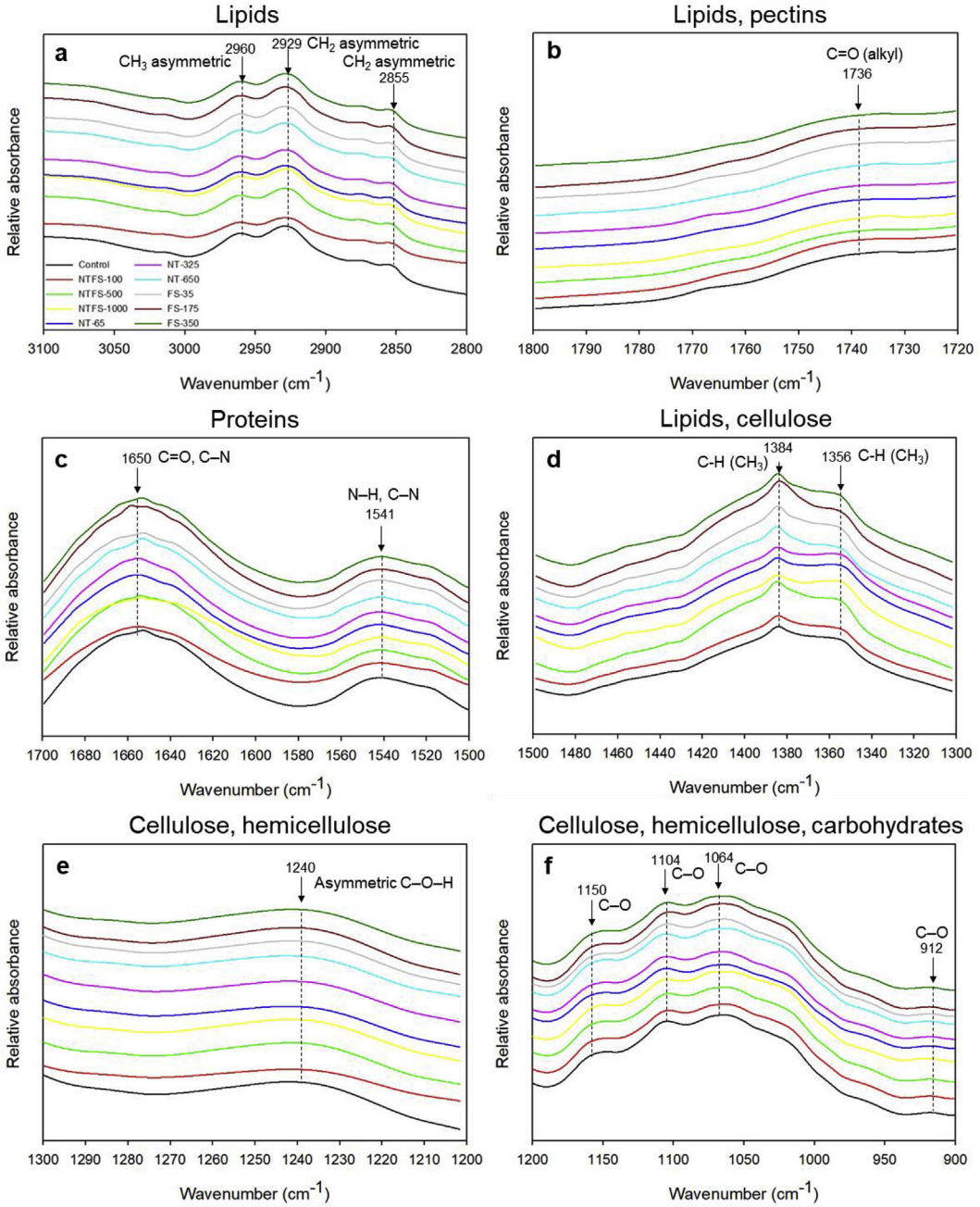

Fig. 4. FTIR spectra of *Arabidopsis* treated with magnetic N-TiO_2/Fe_3O_4@SiO_2 nanophotocatalyst (NTFS), N-TiO_2 (NT), and Fe_3O_4@SiO_2 (FS).

of NTFS in the vascular tissue of plant roots and mesophyll of plant leaves in our study shows a similar uptake pathway to the previous findings: NTFS can be taken up by plant roots and upwards transported from roots to leaves. The plants exposed to NTFS were submerged in the NTFS suspension. The detection of NTFS particles in the epidermis and the mesophyll of plant leaves could be also due to the adsorption and diffusion of NTFS directly through the guard cells in plant leaves. The two possible uptake pathways indicate the bioaccumulation of NTFS and the consequent entrance of NTFS into food-chain.

3.2. Compositional and structural alterations in plant tissues

FT-IR spectroscopy is a well-established tool for the identification of specific functional groups in plant tissues. In this study, FT-IR spectrometry was used to identify any changes in specific functional groups in *Arabidopsis* tissues exposed to NTFS, NT, or FS. Comparisons of FT-IR spectra from *Arabidopsis* tissues treated with different particles at different concentrations are displayed in Fig. 4. Table S2 provides a summary of previously compiled FT-IR data from plant samples that relates the functional groups identified and the macromolecules involved. According to Table S2, the peaks found at 2855, 2929, and 2960 cm^{-1} were assigned to C–H bond in CH_2 and CH_3 asymmetric groups associated with lipids (Dokken and Davis, 2007). The peak at 1736 cm^{-1} (Fig. 4b) was assigned to C=O and COOH groups and identified for lipids and pectins (Dokken and Davis, 2007; Lammers et al., 2009). Fig. 4c shows the peaks at 1541 and 1650 cm^{-1} assigned to the bonds C=O, N–H and C–N identified for proteins (Dokken and Davis, 2007; Rico et al., 2015). The C–H bonds in the CH_3 groups associated with lipids and cellulose were found at 1356 and 1384 cm^{-1} (Fig. 4d) (Sene et al., 1994). The peaks assigned to cellulose and hemicellulose were observed at 1240 and 1072–1040 cm^{-1} in Fig. 4e and f (Rico et al., 2015). Moreover, bonds in carbohydrates were observed from 1200 to 900 cm^{-1} in Fig. 4f (Dokken and Davis, 2007). Based on the FT-IR results, no compositional and structural changes were found in the macromolecules of *Arabidopsis* in different treatments.

Lipids are essential structural components of cell membranes and compose a bilayer matrix for membrane proteins (Miquel et al., 1993). Approximately, 5–10% of plant cell membrane by dry weight were lipids (Ohlrogge and Browse, 1995). Pectins are made of polysaccharides and accountable for the structure of the primary cell wall. Pectins can also bind cells together in the middle lamella (Jarvis, 1992). Hemicellulose and cellulose are the main polysaccharides in primary cell walls and can provide the strength for the primary cell walls. Lignin gives the mechanical support for plant tissues and supplies the rigidity to the cells of terrestrial plants as well (Cabane et al., 2012). Disruption in these macromolecules may lead to changes in morphology and biomass that could impair the normal development of the plants. The fact that no band changes were observed in the FT-IR spectra suggests that exposure to the prepared materials did not cause any negative effects on these macromolecules in *Arabidopsis*, implying the unaffected morphology of plants. Fig. 5 shows the representative *Arabidopsis* plants from each treatment and the fresh and dry biomass of the *Arabidopsis* on the fifth day of exposure to different treatments. The intact morphology and unaffected biomass of the plants confirmed the findings in the FT-IR analysis that NTFS at concentrations ranging from 100 to 1000 mg/L and its two main components (NT and FS) would not cause adverse impacts on plant growth.

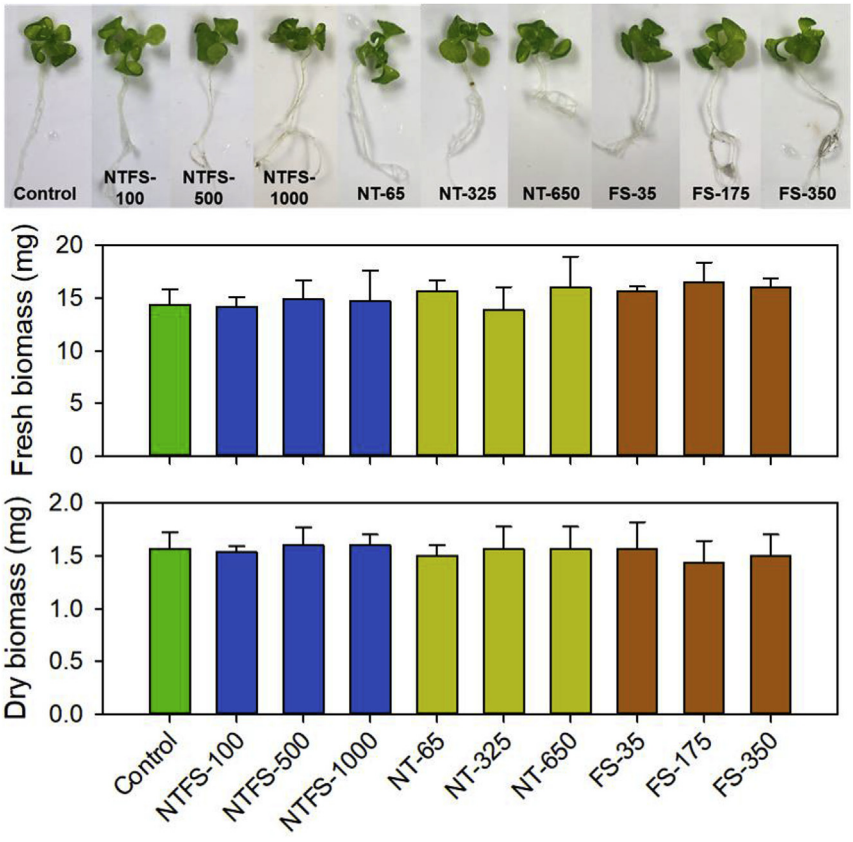

Fig. 5. Representative *Arabidopsis* plants exposed to different particles and the fresh and dry biomass of the plants on the harvest day. Error bars represent standard deviations (n = 3).

Slomberg and Schoenfisch (2012) investigated the phytotoxicity of SiO_2 nanoparticles and found that SiO_2 nanoparticles were not toxic to *Arabidopsis* if adjusting the pH of the growth medium to 5.8. Although the magnetic Fe_3O_4 nanoparticle was reported to be able to induce oxidation stress to plants and affect the growth of plants (Wang et al., 2011), its toxicity could be neutralized by the SiO_2 coating on the particle surface.

3.3. The effect of NTFS on the cytosolic Pi and $MgATP^{2-}$ levels

The cytosolic Pi and $MgATP^{2-}$ levels in the plant cells were calculated through ratiometric analysis and shown in Fig. 6 and Fig. 7. According to the previous studies, the two biosensors can bind to the cytosolic inorganic phosphate and $MgATP^{2-}$, respectively (Mukherjee et al., 2015; De Col et al., 2017). Under excitation condition, the two proteins (Venus and CFP) in the biosensors could emit fluorescence at 465–500 nm (CFP) and 526–561 nm (Venus). By using the Redox Ratio Analysis software, the ratiometric images could be generated from the confocal images and the associated fluorescence resonance energy transfer ratio (Venus/CFP) could be then quantified. A high ratio of Venus to CFP in *Arabidopsis* expressing Pi biosensor implies a low Pi level in plants. On the contrary, a low ratio of Venus to CFP in *Arabidopsis* expressing $MgATP^{2-}$ biosensor indicate a low $MgATP^{2-}$ levels in plants. A low Pi level is usually accompanied by Pi deprivation condition in the plants and a low $MgATP^{2-}$ level indicates a decline of ATP generation. Both conditions could lead to the disruption of the energy supply for the plant growth.

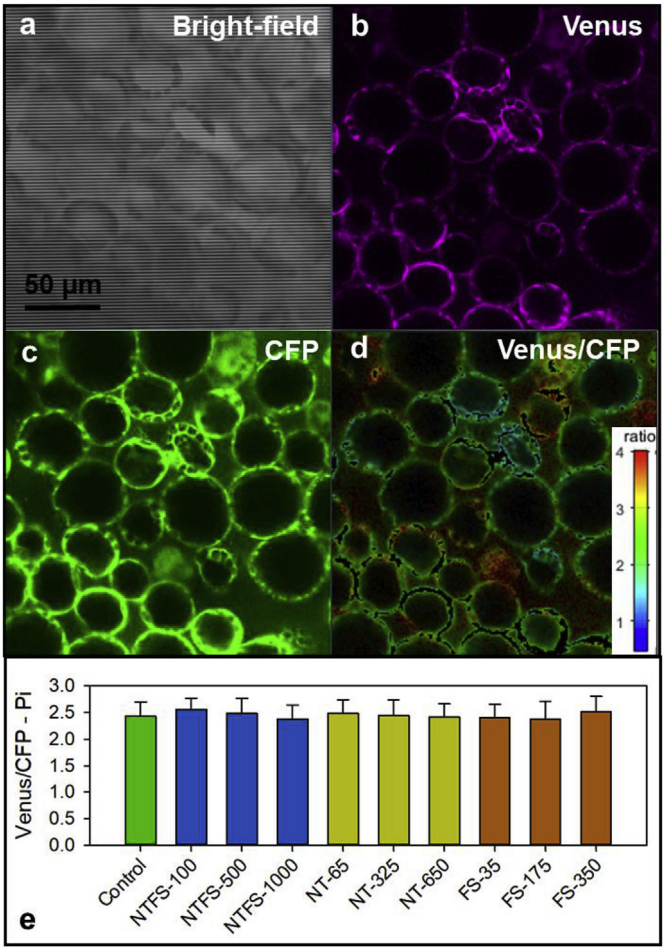

Fig. 6. Bright-field image (a) and confocal microscope images of the *Arabidopsis* seedlings (expressing cytosolic Pi biosensor) showing fluorescence of Venus (b) and CFP (c). The ratio of Venus to CFP is generated as a false-color image (d). (e) Average ratio of Venus to CFP for plants expressing cytosolic Pi biosensor in different treatments. Error bars represent standard deviations (n = 9). (For interpretation of the references to color in this figure legend, the reader is referred to the Web version of this article.)

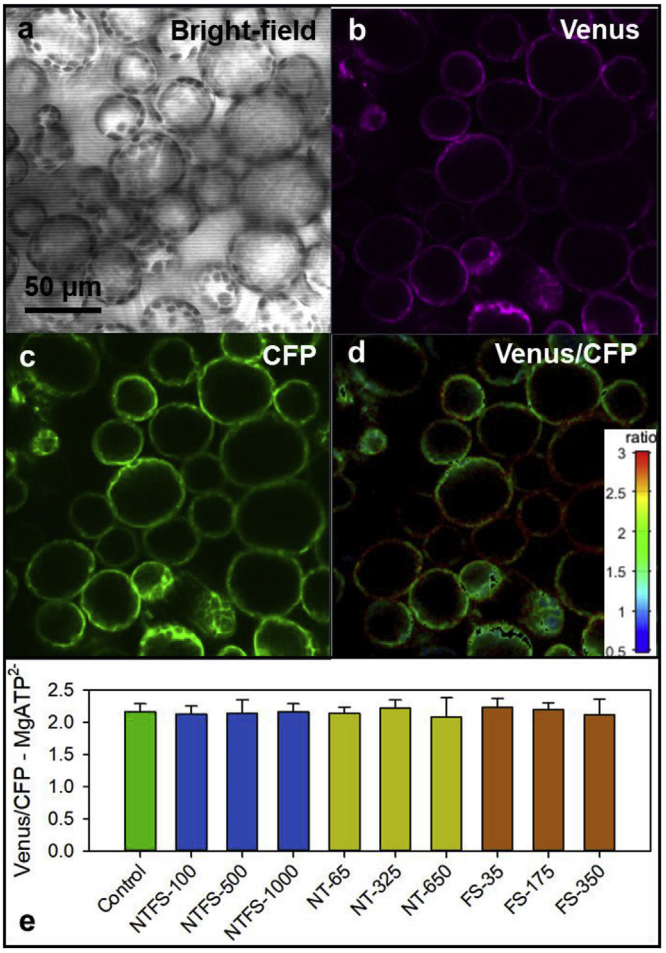

Fig. 7. Bright-field image (a) and confocal microscope images of the *Arabidopsis* seedlings (expressing cytosolic $MgATP^{2-}$ biosensor) showing fluorescence of Venus (b) and CFP (c). The ratio of Venus to CFP is generated as a false-color image (d). (e) Average ratio of Venus to CFP for plants expressing cytosolic $MgATP^{2-}$ biosensor in different treatments. Error bars represent standard deviations (n = 9). (For interpretation of the references to color in this figure legend, the reader is referred to the Web version of this article.)

Phosphorus was acquired and assimilated by plants in inorganic form (Pi) (Schachtman et al., 1998). Insufficient Pi supply could lead to significant low cytosolic Pi level and affect the phosphate-dependent metabolism, such as ATP production (Vance et al., 2003). Thus, the Pi level in cytosol is regularly related to the cytosolic $MgATP^{2-}$ level and plant health. Zahra et al. (2015) proposed that the adsorption of phosphate ions onto TiO_2NPs and the subsequent uptake of TiO_2NPs by the plants, modifications in P speciation by TiO_2NPs, and TiO_2NPs stress on plants in the rhizosphere could all possibly increase the Pi bioavailability and enhance the root exudation (cystine and methionine) of lettuces, which could cause the acidification of rhizosphere soil. All the changes could contribute to the higher Pi uptake by lettuces (Zahra et al., 2015). However, the results shown in Fig. 6e indicate that the cytosolic Pi level in *Arabidopsis* was not affected by NTFS and its two main components at different concentrations. Hong et al. (2005)

reported that TiO_2NPs (5 nm) could improve absorbance and energy transfer efficiency of light (whole chain electron transport) during the photosynthesis in spinach, enhancing the ATP synthesis of plants. Nevertheless, the enhancement of ATP synthesis was not observed in the *Arabidopsis* plants exposed to NTFS and its components at different concentrations (Fig. 7e). The insignificant effects of NTFS on the cytosolic levels of Pi and $MgATP^{2-}$ could be due to the different plant species (*Arabidopsis* vs. lettuce/spinach) and the growth environment (hydroponic system vs. soil system). Another possible reason is the size difference between NTFS and the TiO_2NPs used in previous studies. The size of NTFS (35.12 ± 5.72 nm) is much larger than that of TiO_2NPs (<10 nm) in previous studies, resulting less penetration of the nanoparticles into the plant tissue. The effects of NTFS on the Pi bioavailability and rhizosphere pH were then insignificant and would not cause increasing of the Pi uptake. Moreover, the specific surface area of NTFS is lower than that of smaller TiO_2NPs, leading to the unchanged absorbance and transfer efficiency of light on the thylakoids membrane, and thereby resulting in an insignificant change of cytosolic $MgATP^{2-}$ level in *Arabidopsis*.

The ATP level in plant cells is strongly correlated to the cell membrane integrity and lipid synthesis. A drop in the energy supply could cause extensive hydrolysis of the membrane lipids into free fatty acids and consequential membrane damage (Rawyler et al., 1999). The ATP deprivation could also stop the desaturation of the acyl chains and diminish the lipid synthesis (Rawyler et al., 1999). In this study, the unaffected $MgATP^{2-}$ levels in the plant cells exposed to different nanoparticles were consistent with the results of the FT-IR analysis (Fig. 4a, b and d), which show no chemical changes in the plant lipids. Moreover, the production of ATP is achieved through the breakdown of carbohydrates (e.g. glucose). Thus, the unaffected $MgATP^{2-}$ levels in the plant cells could also support the finding that no chemical changes were detected in the carbohydrates regions of FT-IR spectra (Fig. 4f).

4. Conclusions

This study shows that the magnetic TiO_2-based photocatalyst NTFS can be taken up by *Arabidopsis* roots, penetrate into the vascular tissue, and translocate to the mesophyll of plant leaves. However, the uptake mechanism and potential transformation of NTFS during uptake process are still unclear and worth further investigation. NTFS and its two main components (N-TiO_2 and Fe_3O_4@SiO_2), at concentrations ranging from 0 to 1000 mg/L, did not cause any compositional and structural alterations in the lipids, pectins, proteins, cellulose, hemicellulose, and carbohydrates of the plants. The morphology and biomass of plants were not affected by the NTFS or its components either. By studying the biosensors, the effects of NTFS and its components on the cytosolic Pi and ATP levels were found to be insignificant. The unaffected energy physiology was consistent with the findings of unchanged composition, morphology, and biomass of plants exposed to NTFS. Although this study shows inconsequential toxic effects of NTFS on *Arabidopsis*, further long term studies in soil conditions are necessary for extrapolating the environmental implications of using visible light driven magnetic TiO_2-based photocatalysts. Moreover, NTFS can be taken up by plants, enter the food chain, and potentially ingested by animals and human beings. Numerous research papers have reported that TiO_2-based materials can pass and be absorbed by the mammalian gastrointestinal tract, bioconcentrate, bioaccumulate, and biomagnify in the tissues of mammals and other vertebrates, and cause histopathological and physiological changes in various organs of animals and human beings(Jovanović, 2015). Because the dose makes the poison, the release and disposal of the emerging TiO_2-based materials, which could bioaccumulate in animal and human bodies, should be brought into public's attention.

Conflicts of interest

There are no conflicts to declare.

Acknowledgements

The work was supported by the Research Grants Council of Hong Kong under the General Research Fund (16206214 account). The authors acknowledge Prof. Boon Leong Lim (School of Biological Sciences, the University of Hong Kong, Hong Kong) for providing the *Arabidopsis thaliana* seeds expressing the cytosolic Pi biosensor or the cytosolic $MgATP^{2-}$ biosensor.

Appendix A. Supplementary data

Supplementary data to this article can be found online at https://doi.org/10.1016/j.chemosphere.2019.02.161.

References

Aïssa, A.H., Puzenat, E., Plassais, A., Herrmann, J.-M., Haehnel, C., Guillard, C., 2011. Characterization and photocatalytic performance in air of cementitious materials containing TiO2. Case study of formaldehyde removal. Appl. Catal., B 107, 1–8.

Akpan, U.G., Hameed, B.H., 2009. Parameters affecting the photocatalytic degradation of dyes using TiO2-based photocatalysts: a review. J. Hazard Mater. 170, 520–529.

Álvarez, P.M., Jaramillo, J., Lopez-Pinero, F., Plucinski, P.K., 2010. Preparation and characterization of magnetic TiO2 nanoparticles and their utilization for the degradation of emerging pollutants in water. Appl. Catal., B 100, 338–345.

Asahi, R., Morikawa, T., Irie, H., Ohwaki, T., 2014. Nitrogen-doped titanium dioxide as visible-light-sensitive photocatalyst: designs, developments, and prospects. Chem. Rev. 114, 9824–9852.

Blatnik, J., Luebke, L., Simonet, S., Nelson, M., Price, R., Leek, R., Zeng, L., Wu, A., Brown, E., 2012. Dye surface coating enables visible light activation of TiO2 nanoparticles leading to degradation of neighboring biological structures. Microsc. Microanal. 18, 134–142.

Burda, C., Lou, Y., Chen, X., Samia, A.C., Stout, J., Gole, J.L., 2003. Enhanced nitrogen doping in TiO2 nanoparticles. Nano Lett. 3, 1049–1051.

Cabane, M., Afif, D., Hawkins, S., 2012. Lignins and abiotic stresses. Adv. Bot. Res. 61, 219–262.

Carpita, N., Sabularse, D., Montezinos, D., Delmer, D.P., 1979. Determination of the pore size of cell walls of living plant cells. Science 205, 1144–1147.

Chalasani, R., Vasudevan, S., 2013. Cyclodextrin-functionalized Fe3O4@TiO2: reusable, magnetic nanoparticles for photocatalytic degradation of endocrine-disrupting chemicals in water supplies. ACS Nano 7, 4093–4104.

Chen, W.J., Tsai, P.J., Chen, Y.C., 2008. Functional Fe3O4/TiO2 core/shell magnetic nanoparticles as photokilling agents for pathogenic bacteria. Small 4, 485–491.

Chen, X., Burda, C., 2008. The electronic origin of the visible-light absorption properties of C-, N-and S-doped TiO2 nanomaterials. J. Am. Chem. Soc. 130, 5018–5019.

De Col, V., Fuchs, P., Nietzel, T., Elsässer, M., Voon, C.P., Candeo, A., Seeliger, I., Fricker, M.D., Grefen, C., Møller, I.M., 2017. ATP sensing in living plant cells reveals tissue gradients and stress dynamics of energy physiology. eLife 6, e26770.

Dokken, K.M., Davis, L.C., 2007. Infrared imaging of sunflower and maize root anatomy. J. Agric. Food Chem. 55, 10517–10530.

Dokken, K.M., Davis, L.C., Marinkovic, N.S., 2005. Use of infrared microspectroscopy in plant growth and development. Appl. Spectrosc. Rev. 40, 301–326.

Fricker, M.D., 2016. Quantitative redox imaging software. Antioxidants Redox Signal. 24, 752–762.

Ghosh, M., Bandyopadhyay, M., Mukherjee, A., 2010. Genotoxicity of titanium dioxide (TiO 2) nanoparticles at two trophic levels: plant and human lymphocytes. Chemosphere 81, 1253–1262.

Herrmann, J.-M., Disdier, J., Pichat, P., Malato, S., Blanco, J., 1998. TiO2-based solar photocatalytic detoxification of water containing organic pollutants. Case studies of 2, 4-dichlorophenoxyaceticacid (2, 4-D) and of benzofuran. Appl. Catal., B 17, 15–23.

Hong, F., Zhou, J., Liu, C., Yang, F., Wu, C., Zheng, L., Yang, P., 2005. Effect of nano-TiO2 on photochemical reaction of chloroplasts of spinach. Biol. Trace Elem. Res. 105, 269–279.

Jarvis, M., 1992. Control of thickness of collenchyma cell walls by pectins. Planta 187, 218–220.

Jovanović, B., 2015. Critical review of public health regulations of titanium dioxide, a human food additive. Integrated Environ. Assess. Manag. 11, 10–20.

Klančnik, K., Drobne, D., Valant, J., Koce, J.D., 2011. Use of a modified Allium test with nanoTiO2. Ecotoxicol. Environ. Saf. 74, 85–92.
Knowles, J.R., 1980. Enzyme-catalyzed phosphoryl transfer reactions. Annu. Rev. Biochem. 49, 877–919.
Kumar, A., Khan, M., Fang, L., Lo, I.M.C., 2017. Visible-light-driven N-TiO2@SiO2@Fe3O4 magnetic nanophotocatalysts: synthesis, characterization, and photocatalytic degradation of PPCPs. J. Hazard Mater. https://doi.org/10.1016/j.jhazmat.2017.07.048.
Kurepa, J., Paunesku, T., Vogt, S., Arora, H., Rabatic, B.M., Lu, J., Wanzer, M.B., Woloschak, G.E., Smalle, J.A., 2010. Uptake and distribution of ultrasmall anatase TiO2 Alizarin red S nanoconjugates in Arabidopsis thaliana. Nano Lett. 10, 2296–2302.
Lammers, K., Arbuckle-Keil, G., Dighton, J., 2009. FT-IR study of the changes in carbohydrate chemistry of three New Jersey pine barrens leaf litters during simulated control burning. Soil Biol. Biochem. 41, 340–347.
Larue, C., Laurette, J., Herlin-Boime, N., Khodja, H., Fayard, B., Flank, A.-M., Brisset, F., Carriere, M., 2012a. Accumulation, translocation and impact of TiO2 nanoparticles in wheat (Triticum aestivum spp.): influence of diameter and crystal phase. Sci. Total Environ. 431, 197–208.
Larue, C., Veronesi, G., Flank, A.-M., Surble, S., Herlin-Boime, N., Carrière, M., 2012b. Comparative uptake and impact of TiO2 nanoparticles in wheat and rapeseed. J. Toxicol. Environ. Health, A 75, 722–734.
Lei, Z., Mingyu, S., Chao, L., Liang, C., Hao, H., Xiao, W., Xiaoqing, L., Fan, Y., Fengqing, G., Fashui, H., 2007. Effects of nanoanatase TiO2 on photosynthesis of spinach chloroplasts under different light illumination. Biol. Trace Elem. Res. 119, 68–76.
Ma, C., Liu, H., Chen, G., Zhao, Q., Eitzer, B., Wang, Z., Cai, W., Newman, L.A., White, J.C., Dhankher, O.P., 2017. Effects of titanium oxide nanoparticles on tetracycline accumulation and toxicity in Oryza sativa (L.). Environ. Sci. Nano 4, 1827–1839.
Miquel, M., James, D., Dooner, H., 1993. Arabidopsis requires polyunsaturated lipids for low-temperature survival. Proc. Natl. Acad. Sci. Unit. States Am. 90, 6208–6212.
Monica, R.C., Cremonini, R., 2009. Nanoparticles and higher plants. Caryologia 62, 161–165.
Mudunkotuwa, I.A., Anthony, T.R., Grassian, V.H., Peters, T.M., 2016. Accurate quantification of TiO2 nanoparticles collected on air filters using a microwave-assisted acid digestion method. J. Occup. Environ. Hyg. 13, 30–39.
Mukherjee, P., Banerjee, S., Wheeler, A., Ratliff, L.A., Irigoyen, S., Garcia, L.R., Lockless, S.W., Versaw, W.K., 2015. Live imaging of inorganic phosphate in plants with cellular and subcellular resolution. Plant Physiol. 167, 628–638.
Murashige, T., Skoog, F., 1962. A revised medium for rapid growth and bio assays with tobacco tissue cultures. Physiol. Plantarum 15, 473–497.
Nair, R., Varghese, S.H., Nair, B.G., Maekawa, T., Yoshida, Y., Kumar, D.S., 2010. Nanoparticulate material delivery to plants. Plant Sci. 179, 154–163.
Ohlrogge, J., Browse, J., 1995. Lipid biosynthesis. Plant Cell 7, 957.
Puchtler, H., Meloan, S.N., Terry, M.S., 1969. On the history and mechanism of alizarin and alizarin red S stains for calcium. J. Histochem. Cytochem. 17, 110–124.
Rao, T.N., Tryk, D.A., Fujishima, A., 2007. Applications of TiO2 photocatalysis. Encycl. Electrochem.: Online 536–560.
Rawyler, A., Pavelic, D., Gianinazzi, C., Oberson, J., Braendle, R., 1999. Membrane lipid integrity relies on a threshold of ATP production rate in potato cell cultures submitted to anoxia. Plant Physiol. 120, 293–300.
Rico, C.M., Peralta-Videa, J.R., Gardea-Torresdey, J.L., 2015. Differential effects of cerium oxide nanoparticles on rice, wheat, and barley roots: a Fourier Transform Infrared (FT-IR) microspectroscopy study. Appl. Spectrosc. 69, 287–295.
Schachtman, D.P., Reid, R.J., Ayling, S.M., 1998. Phosphorus uptake by plants: from soil to cell. Plant Physiol. 116, 447–453.
Schneider, J., Matsuoka, M., Takeuchi, M., Zhang, J., Horiuchi, Y., Anpo, M., Bahnemann, D.W., 2014. Understanding TiO2 photocatalysis: mechanisms and materials. Chem. Rev. 114, 9919–9986.
Seeger, E.M., Baun, A., Kästner, M., Trapp, S., 2009. Insignificant acute toxicity of TiO2 nanoparticles to willow trees. J. Soils Sediments 9, 46–53.
Sene, C.F., McCann, M.C., Wilson, R.H., Grinter, R., 1994. Fourier-transform Raman and Fourier-transform infrared spectroscopy (an investigation of five higher plant cell walls and their components). Plant Physiol. 106, 1623–1631.
Slomberg, D.L., Schoenfisch, M.H., 2012. Silica nanoparticle phytotoxicity to Arabidopsis thaliana. Environ. Sci. Technol. 46, 10247–10254.
Song, U., Jun, H., Waldman, B., Roh, J., Kim, Y., Yi, J., Lee, E.J., 2013. Functional analyses of nanoparticle toxicity: a comparative study of the effects of TiO2 and Ag on tomatoes (Lycopersicon esculentum). Ecotoxicol. Environ. Saf. 93, 60–67.
Thurn, K.T., Paunesku, T., Wu, A., Brown, E., Lai, B., Vogt, S., Maser, J., Aslam, M., Dravid, V., Bergan, R., 2009. Labeling TiO2 nanoparticles with dyes for optical fluorescence microscopy and determination of TiO2–DNA nanoconjugate stability. Small 5, 1318–1325.
Vance, C.P., Uhde-Stone, C., Allan, D.L., 2003. Phosphorus acquisition and use: critical adaptations by plants for securing a nonrenewable resource. New Phytol. 157, 423–447.
Vautier, M., Guillard, C., Herrmann, J.-M., 2001. Photocatalytic degradation of dyes in water: case study of indigo and of indigo carmine. J. Catal. 201, 46–59.
Wang, H., Kou, X., Pei, Z., Xiao, J.Q., Shan, X., Xing, B., 2011. Physiological effects of magnetite (Fe3O4) nanoparticles on perennial ryegrass (Lolium perenne L.) and pumpkin (Cucurbita mixta) plants. Nanotoxicology 5, 30–42.
Xu, Y.-J., Zhuang, Y., Fu, X., 2010. New insight for enhanced photocatalytic activity of TiO2 by doping carbon nanotubes: a case study on degradation of benzene and methyl orange. J. Phys. Chem. C 114, 2669–2676.
Xuan, S., Jiang, W., Gong, X., Hu, Y., Chen, Z., 2008. Magnetically separable Fe3O4/TiO2 hollow spheres: fabrication and photocatalytic activity. J. Phys. Chem. C 113, 553–558.
Zahra, Z., Arshad, M., Rafique, R., Mahmood, A., Habib, A., Qazi, I.A., Khan, S.A., 2015. Metallic nanoparticle (TiO2 and Fe3O4) application modifies rhizosphere phosphorus availability and uptake by Lactuca sativa. J. Agric. Food Chem. 63, 6876–6882.
Zhang, W., Lo, I.M.C., Hu, L., Voon, C.P., Lim, B.L., Versaw, W.K., 2018. Environmental risks of nano zero-valent iron for arsenate remediation: impacts on cytosolic levels of inorganic phosphate and MgATP2-in Arabidopsis thaliana. Environ. Sci. Technol. 52, 4385–4392.